Supplementary information

Polarization–preservation analysis for robust reflection-mode optical glucose sensing in turbid media

Hsin-Yi Hsieh[a,*], Chia-Chun Chang[a] and Chin-Chuan Hsieh[a]

[a]VisEra Technologies Company Ltd., No. 12, Dusing Rd. 1, Hsinchu Science Park, Taiwan 30078

*Correspondence: hy_hsieh@viseratech.com; Tel.: +886-3-6668788 ext.5260

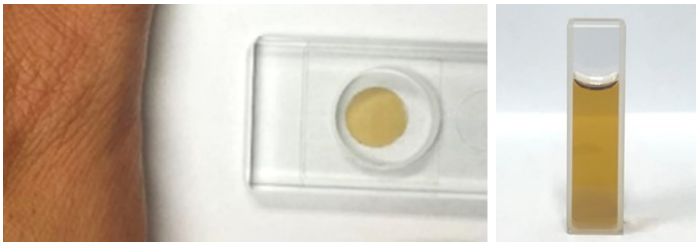

Figure S1. Visual comparison of human skin tone and pigment-containing phantoms used in this study. (Left) Photograph of human skin under ambient illumination as a visual reference. (Middle) Two-layer skin-mimicking phantom showing the upper layer containing a 0.3% pigment solution. (Right) Cuvette containing a 0.01% pigment solution used for background absorption characterization in the cuvette-based measurements.

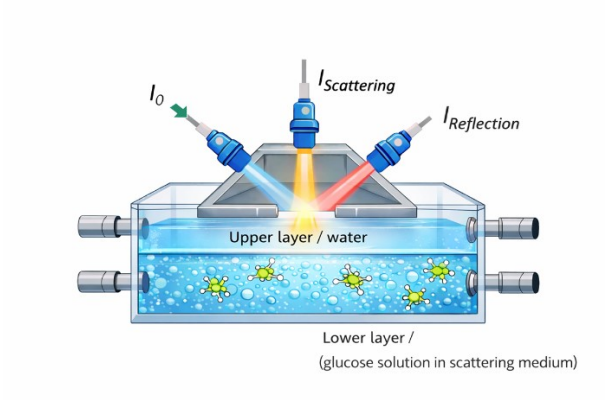

Figure S2. Schematic illustration of the reflection-mode trapezoid-holder configuration used for non-polarized scattering and reflection measurements.

Incident light (I_0) was introduced through the 45° port, while the scattered ($I_{Scattering}$) and reflected ($I_{Reflection}$) signals were collected through the 90° and 135° detection ports, respectively. The upper layer represents water, whereas the lower layer consists of a glucose solution in a scattering medium.

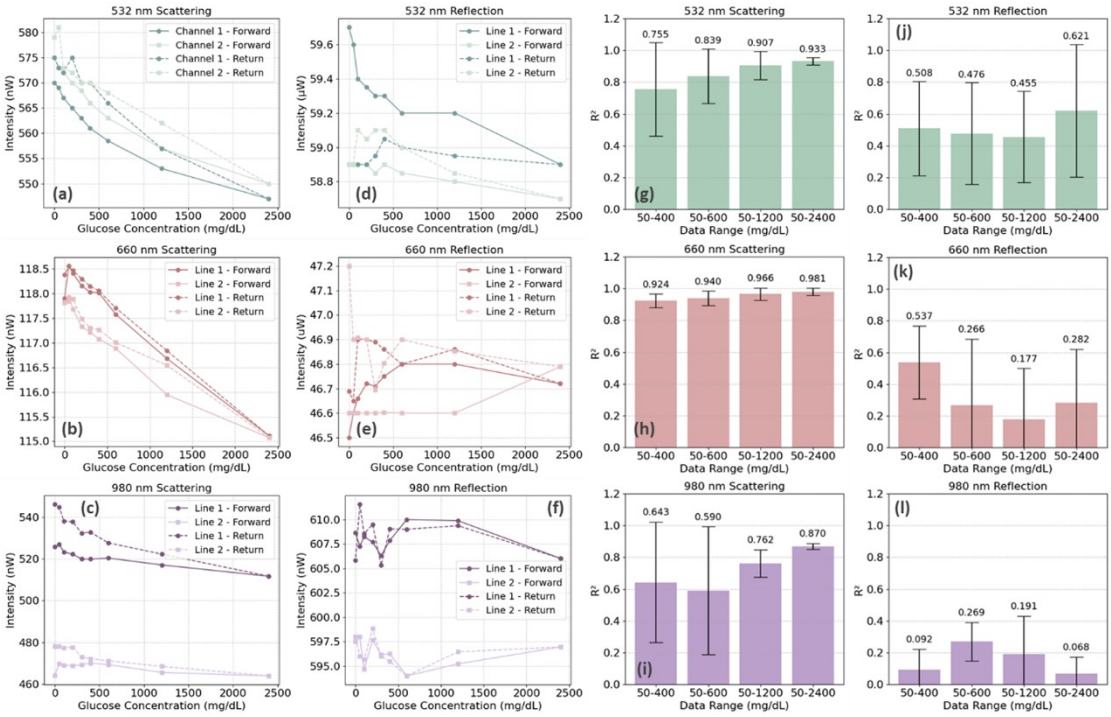

Figure S3. Complete non-polarized reflection-mode scattering and reflection responses measured using the trapezoid-holder configuration. (a–c) Non-polarized scattering intensity as glucose concentration was increased from 0 to 2400 mg/dL (forward) and subsequently decreased from 2400 to 0 mg/dL (backward). (d–f) Corresponding non-polarized reflection intensity under the same forward and backward concentration cycling. (g–i) Linear regression analysis of non-polarized scattering responses over extended glucose concentration ranges. (j–l) Linear regression analysis of non-polarized reflection responses over the same concentration ranges.

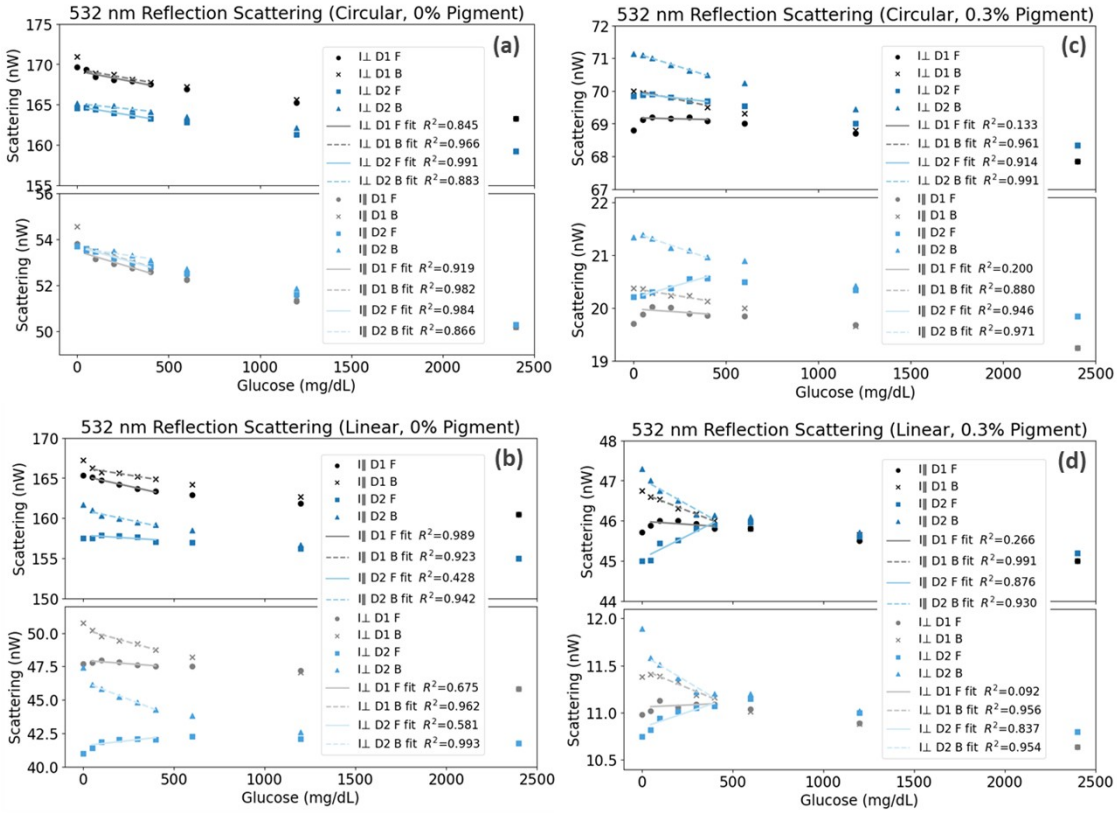

Figure S4. Reflection-mode polarization-resolved scattering responses at 532 nm under non-pigmented (0%) and pigment-interference (0.3%) conditions.

Circular and linear co-polarized ($I_{//}$) and cross-polarized ($I_{\perp}$) scattering intensities are shown as functions of glucose concentration during forward and backward cycling. Linear regression analysis was performed over the physiological concentration range (50–400 mg/dL). These data provide supporting evidence for wavelength-dependent polarization behavior corresponding to the summary correlation values presented in Table 2.

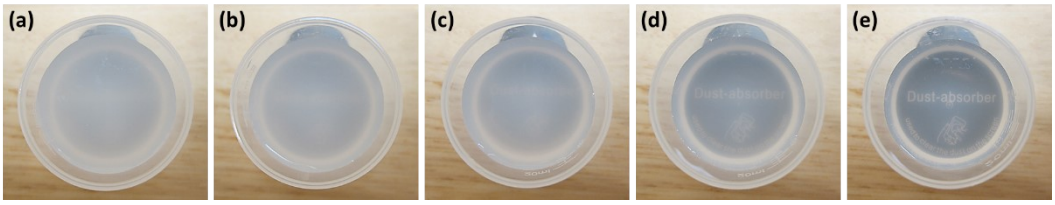

Figure S5. Visual demonstration of glucose-induced reduction in turbidity in a milk-based scattering phantom. A milk solution (0.5 mL milk in 100 mL water) was prepared with increasing D-glucose concentrations: (a) 0 mg/dL, (b) 2500 mg/dL, (c) 5000 mg/dL, (d) 10000 mg/dL, and (e) 20000 mg/dL. As glucose concentration increases, the solution becomes progressively more transparent, allowing improved visibility of the background text. This behavior reflects the reduction in scattering due to refractive index matching between the scattering particles (casein micelles and lipid globules) and the surrounding medium. The result provides a qualitative illustration of glucose-induced modulation of scattering in turbid media. Note that these concentrations are higher than physiological levels and are used here for visual demonstration of the refractive index matching effect.

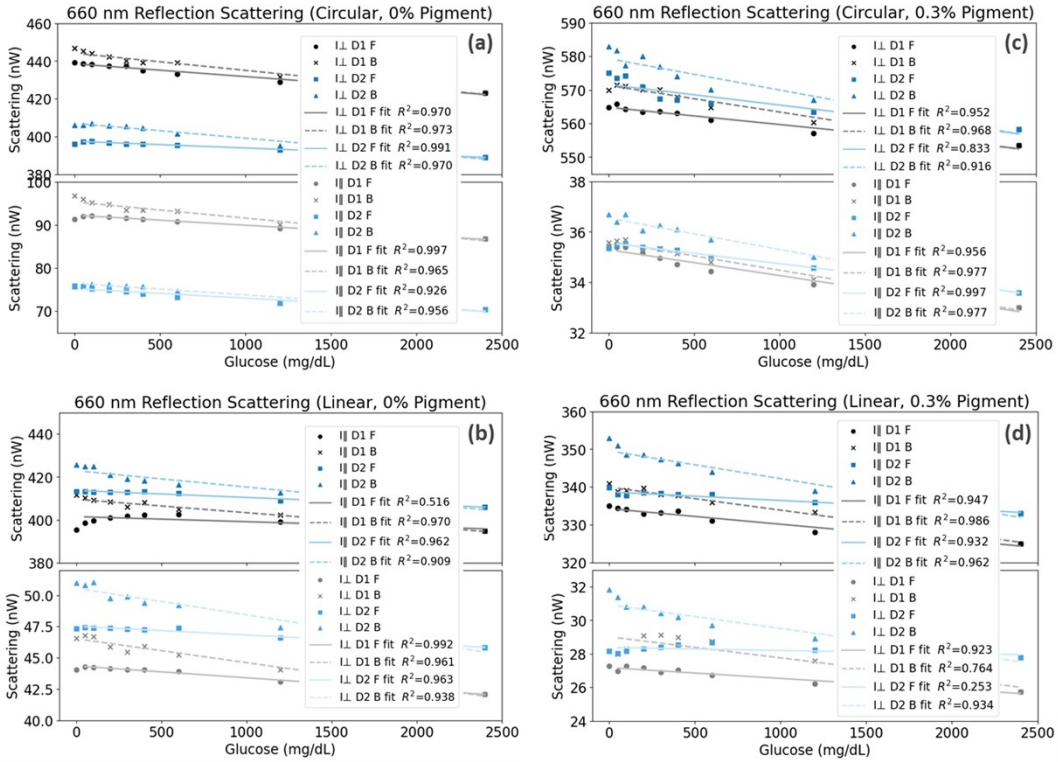

Figure S6. Full-range regression analysis of reflection-mode polarization-resolved scattering at 660 nm over an extended glucose concentration range (0–2400 mg/dL).

Co-polarized ($I_{//}$) and cross-polarized ($I_{\perp}$) intensities were analyzed under non-pigmented (0%) and pigment-interference (0.3%) conditions. Linear regression fits were performed across the full concentration range to assess trend continuity beyond the physiological window (50–400 mg/dL). These results provide supplementary evaluation of polarization-resolved behavior at elevated glucose concentrations.